Renewable Energy 90 (2016) 430–439

Contents lists available at ScienceDirect

Renewable Energy

journal homepage: www.elsevier.com/locate/renene

Optimal management of microgrids including renewable energy scources using GPSO-GM algorithm

Mohammad Abedini [a], Mohammad H. Moradi [a, *], S. Mahdi Hosseinian [b]

[a] Department of Electrical Engineering, Faculty of Engineering, Bu-Ali Sina University, Hamedan, Iran
[b] Department of Civil Engineering, Faculty of Engineering, Bu-Ali Sina University, Hamedan, Iran

ARTICLE INFO

Article history:
Received 18 August 2015
Received in revised form
10 December 2015
Accepted 2 January 2016
Available online xxx

Keywords:
Microgrid
Renewable energy resources
Optimization
Wind generation
Photovoltaic (PV)

ABSTRACT

Environmentally friendly energy sources with high power quality or reliability and low costs are regarded as an effective solution for energy supply problems arising from use of conventional methods. Presented in this paper, gives an optimal management strategy of PV/wind/diesel independent hybrid systems for supplying required energy in autonomous microgrids. A new optimization problem is formulated for minimizing the capital investment and fuel costs of the system. To solve the proposed optimization problem a novel algorithm, named Guaranteed convergence Particle Swarm Optimization with Gaussian Mutation (GPSO-GM), is developed. Two operators, namely mutation and guaranteed convergence, are added to PSO in order to help finding more accurate results and increasing the speed of calculations. The performance of the proposed strategy is evaluated in two case studies.

1. Introduction

A microgrid is seen as an interconnection of distributed generations (DGs) which is integrated with electrical and thermal loads as well as energy storages, and it operates as a single small scale system in low-voltage distribution systems. In microgrids, power quality, reliability, and security can be enhanced by the use of power electronic interfaces and controls [1,2]. A microgrid might operate in grid-connected or islanded modes. In a grid-connected mode, the voltage and frequency of microgrids are dictated by the main grid while in an islanded mode controlling DG units along with managing active and reactive power are considered for regulating voltage and frequency [3,4].

In microgrides, renewable energy sources (RESs) might be used in different types and sizes, and different forms, for example, isolated or grid connected, single or hybrid [5]. Reference [8] suggests PV panels and wind turbines as a preferred choice for the energy supply problem due to their accessibility and inexhaustibility. The studies of [6,7] conclude that hybrid renewable energy sources (systems) should be considered as an economical and reliable solution for the energy supply problem particularly in remote areas where a high reliable power is needed and access to the grid is difficult [9]. Similarly, the study of [10] argues that in remote areas hybrid PV-diesel systems are competitive with diesel generation because of high costs involved in the energy supply of diesel.

Many researchers have looked at the use of hybrid systems with renewable energy sources [11,12]. For instance, the study of [13] explores the feasibility of small hydro-PV-wind hybrid systems in an islanded rural area of Dijon district of Ethiopia. In the same vein, the research of [14] examines the implementation of hybrid power systems for a village in Saudi Arabia and suggests such systems as a feasible solution with energy cost of 0.212 US$/kWh. Reference [15] proposes an optimal hybrid solar-wind energy system, and similarly Reference [16] looks at sizing and economic problems of autonomous hybrid solar-wind energy systems. The study of [19], talks about an optimal pumped hydro storage system as a promising technology for standalone photoelectric energy penetration for small autonomous systems in remote areas, and the reach of [20] explores the sizing problem of integrated solar-wind systems with battery storages. The authors of [21] write on the effect of grid dependency on the integration of renewable subunits and the authors of [22] discuss technical and operational issues of solar and wind generation in distribution networks.

In practice, finding an optimal design and operation of hybrid energy systems simultaneously are problematic and few studies have looked at this problem despite its widespread nature.

* Corresponding author.
E-mail addresses: m_abedini_dr@yahoo.com (M. Abedini), mh_moradi@yahoo.co.uk (M.H. Moradi), s.hosseinian@basu.ac.ir (S.M. Hosseinian).

http://dx.doi.org/10.1016/j.renene.2016.01.014
0960-1481/

Therefore, it is required to provide an effective strategy for evaluating optimal capacity and operation of sources and storages in hybrid energy systems. This paper addresses this knowledge gap via establishing an optimization method for finding the optimal capacity and operation of sources and storages simultaneously in a hybrid system over its lifespan in which the capital investment and operation costs are minimized. In doing so, a novel optimization problem is formulated and an innovative algorithm, named GPSO-GM, is developed to solve the proposed optimization problem. In addition, to run GPSO-GM a load flow algorithm is developed. The output of the optimization method identifies optimal capacity and hourly generation of the sources and storages over their lifespan in a hybrid system. The proposed strategy demonstrates that hybrid systems are an effective solution for supply problems of island microgrids from financial and practical aspects, particularly in remote areas where there is no access to a grid.

The rest of the paper is organized as follows. Firstly, the mathematical modeling of subsystems used in a hybrid system is given. Then the proposed problem formulation and its corresponding solution are provided. Finally, the simulation results and discussion are presented.

2. Mathematical modeling of subsystems

For modeling let consider a hybrid energy system with four subsystems (modules), namely PV panels and wind turbines (renewable energy sources), batteries (storage devices), and diesel generators [5]. Mathematical modeling of these subsystems can be outlined as follows.

2.1. PV panels

Different types of PV panels with different characteristics and costs might be considered for modeling. In a simple model, the power output of a PV panel can be determined by Ref. [23],

$$P^{PV}(t) = I_r(t) \times S \times \eta^{PV} \times \eta_{inv} \tag{1}$$

Unfortunately, (1) does not consider the temperature effect as, for example, a temperature rise adversely affects the efficiency of PV panels. To consider the effective of temperature on the output power of a PV panel, the following equation might be used [23],

$$P^{PV}(t) = P^{PV}_{st} \times f^{PV} \times \left(\frac{I_r(t)}{I_{r,st}}\right) \times \left(1 + \alpha^{PV}\left[T_C(t) - T_{C,st}(t)\right]\right) \tag{2}$$

2.2. Wind turbines

The power output of wind turbines can be calculated based on the wind speed, at the hub height, and the output characteristics of the wind turbine generator. A piece-vice linear function might be employed for calculating the hourly power output of a wind generator, as shown in Fig. 1 [12],

$$P_{w,j}(t) = \begin{cases} 0 & v_j < v_{ci,j} \\ P^{rated}_{w,j} \cdot \dfrac{v_j(t) - v_{ci,j}}{v^{rated}_j - v_{ci,j}} & v_{ci,j} \le v_j(t) < v^{rated}_j \\ P^{rated}_{w,j} & v^{rated}_j \le v_j(t) < v_{co,j} \\ 0 & v_{co,j} \le v_j(t) \end{cases} \tag{3}$$

The wind speed at the hub height can be calculated by use of power-law equation (4) if the wind speed is available in the reference height (h_r) [24].

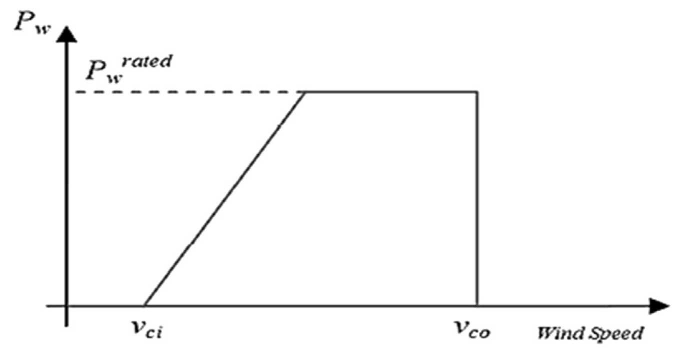

Fig. 1. Typical piece-vice approximation of wind turbine power output.

$$v(t) = v_r(t) \cdot \left(\frac{h}{h_r}\right)^{\gamma} \tag{4}$$

2.3. Battery banks

Battery banks are typically utilized as an energy storage unit. There follows the difference between power generated by RESs, and load determines whether the battery banks should be charged or discharged. During charging and discharging processes, the state of charge (SOC) limitation should be applied, as given by Refs. [25],

$$SOC_{\min,k} \le SOC_k(t) \le SOC_{\max,k} \tag{5}$$

In the case where batteries are connected in series, as assumed in this paper, to supply the desired DC operating voltage, considered to be 380 V in this paper, the number of batteries can be calculated by,

$$N_{battery,s} = \frac{V_{DC}}{V^{rated}_{battery}} \tag{6}$$

2.4. Diesel generators

In grid-independent hybrid systems, the sum of power generated by RESs and stored in battery banks might not meet the load demand so independent power sources, as a backup, such as fuel cell systems or diesel generators, are required in such circumstances. For this purpose diesel generators are selected in this paper because of the medium size of the considered energy system. The size and type of diesel generators are typically dependent on the nature of the supplied load. To find the optimal capacity of a diesel generator, Reference [26] suggests to considering that the diesel generator is directly connected to the load and it is therefore required to supply the whole load. Accordingly the size of the generator needs to be equal to the maximum demand. This, however, is not optimal. In this study, the capacity of the diesel generator is treated as an optimization variable which needs to be determined based on its installation and operational costs in comparison with the cost involved in reinforcing the RESs and battery banks.

3. Optimization problem formulation

Let consider a hybrid energy system with above four subsystems. Let also consider that the diesel generators are designed for providing backup in the case where the renewable energy resources and battery banks are not able to supply the whole electric power. The cost of this hybrid energy system can be calculated based on three components, namely installation, maintenance and operating costs. The sum of cost components, denoted by f, of the four subsystems is defined as the objective function, and can be calculated by,

$$f = \min\left(C_{invs}^{Total} + C_{ope\&main}^{Total}\right) \tag{7}$$

where C_{invs}^{Total} is the capital investment costs comprising installation, construction, and equipment costs, as given by,

$$C_{invs}^{Total} = \sum_{m=1}^{N_{diesel}} P_{diesel_m} \times c_{inv}^{diesel} + \sum_{m=1}^{N_{battery}} P_{battery_m} \times c_{inv}^{battery} + \sum_{m=1}^{N_{pv}} P_{pv_m} \times c_{inv}^{pv} + \sum_{m=1}^{N_{wind}} P_{wind_m} \times c_{inv}^{pv} \tag{8}$$

and $C_{ope\&main}^{Total}$ is the operation and maintenance costs including fuel, repair, inspection, labor and alike costs. The present worth of such costs can be calculated by,

$$C_{ope\&main}^{Total} = \sum_{n=1}^{Nyr} \sum_{t=1}^{T} \left\{ \sum_{m=1}^{N_{wind}} \Delta_t \times P_{wind_m,t} \times C_{wind} + \sum_{m=1}^{Npv} \Delta_t \times P_{pv_m,t} \times C_{pv} + \sum_{m=1}^{N_{battery}} \Delta_t \times P_{battery_m,t} \times C_{battery} + \sum_{m=1}^{N_{diesel}} \Delta_t \times P_{diesel_m,t} \times C_{diesel} \right\} \left(\frac{1+InfR}{1+IntR}\right)^n \tag{9}$$

3.1. Constraints

Some constraints involved in the optimization problem as outlined below.

1. *Power flow constraint*

Active and reactive power generation should be equal to load at all buses [22],

$$P_{gi,t} = P_{loadi,t} + P_{i,t}^{RES} \pm P_{battery} + V_{i,t} \sum_{j=1}^{NB} V_{j,t} Y_{j,t} \cos\left(\delta_{i,t} - \delta_{j,t} - \theta_{j,t}\right) \tag{10}$$

2. *Voltage constraint*

Voltage magnitudes should be kept within the required ranges [12],

$$V_{\min} \le V_i \le V_{\max} \tag{11}$$

3. *Current constraint*

Current flow values in microgrid lines should be less than their acceptable values [18],

$$I_i \le I_i^{\max} \quad i = 1, \ldots, N_{Br} \tag{12}$$

4. *Generation constraint*

Generated power of RESs in period t should be kept within minimum and maximum power limits [18],

$$P_{\min}^{RES} \le P_{i,t}^{RES} \le P_{\max}^{RES} \tag{13}$$

4. Problem solution

This part develops an innovative solution for the above proposed optimization problem, as depicted in Fig. 2, which is based on a new algorithm, named GPSO-GM, discussed later. The process of the solution begins with initializing the optimization problem and parameters of the mutation, which is followed by initiating the crossover. For each solution, the simulation is performed in an hourly basis of operation. Then iterations in simulation start with calculating the power generation of PV panels and wind turbines using wind speed and solar irradiance data. Next P_{Dif} is calculated by,

$$P_{Dif} = P_{load} - \left(P_{pv} + P_{Wind}\right) \tag{14}$$

A negative value for P_{Dif} is meant that the renewable resources are able to supply the load and there is an extra power that needs to be stored in the battery banks. A positive value for P_{Dif}, however, is meant that renewable resources are not enough to supply the load; that is there is a power shortage. To deal with this power shortage the strategy is to use the power stored in the battery banks taking into account the SOC_{Min} limitation of the battery banks. In the case where the power provided by the battery banks is not sufficient, a diesel generator is also considered for providing the extra power required. This process can mathematically be formulated as, see Fig. 2 also,

$$\begin{cases} P_{Dif} - \left(P_{Battery} - SOC_{Min}\right) < 0 & \ldots \text{using batteries} \\ P_{Dif} - \left(P_{Battery} - SOC_{Min}\right) > 0 & \ldots \text{using batteries and generators} \end{cases} \tag{15}$$

There follows the hourly output power of the diesel generator can be calculated. Notably, the maximum power output of the diesel generator is selected as its capacity. In this stage of the iteration, all the optimization variables are determined and, therefore, the objective function can then be calculated. This is followed by updating GPSO-GM and if the termination criterion is met the process is ended otherwise the next iteration is started.

There are a number of matters considered in the process of obtaining the optimal solution as outlined in the following:

- The time simulation is performed for one day of each month. Therefore 12 days are considered, each representing one month, so for each year 284 iterations are considered for modeling the annual load of the system.
- For the illustration purpose, the efficiency of regulators and converters are not shown in equations of the flowchart, presented in Fig. 2, but they are considered in the simulations.
- In order to have an appropriate financial consideration, interest and inflation rates are considered to calculate the net present values of different costs based on their occurrence time.
- The constraints considered in the simulations, as discussed before, include satisfaction of the power demand; wind turbine; battery bank SOC; and PV panel maximum output constraints.

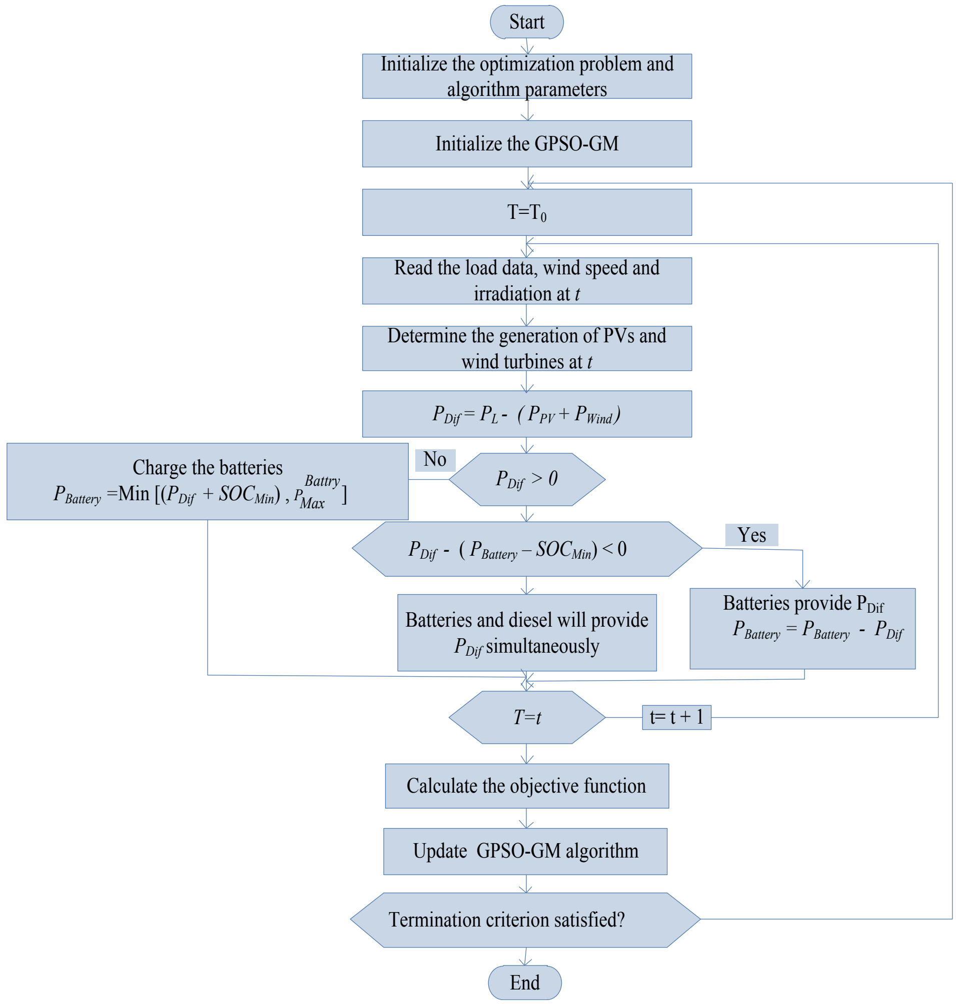

Fig. 2. Conceptual flowchart of the proposed operation strategy.

4.1. Proposed GPSO-GM algorithm

To solve the proposed optimization problem, an innovative algorithm is developed using the PSO method. PSO is a fast method, compared with other evolutionary methods; however, it may converge to a local minimum value which might not necessary be an optimal global solution and even rising iteration numbers is not able to cope with such global convergence problem. As a consequence, in practice, it might be hard to validate the solution derived by PSO. In an attempt to address this validation problem, the study of [27] suggests adding a guaranteed convergence operator to PSO to make the convergence of solutions possible. Unfortunately, this globally improved algorithm, called GPSO, fails to deal with problems involving a small searching region because of the PSO information sharing mechanism. In order to address this shortfall, this paper develops the GPSO algorithm by adopting a Gaussian mutation operator which assists in finding the optimal global solution. This new algorithm is named GPSO-GM and its scheme is outlined as follows.

Step 1: *Initialization:* Set $t = 0$ and randomly make m swarms (batteries, PV panels and wind turbines), [$y_i(0)$,i = 1,...,m].For each swarm, set $y_i^*(0) = y_i(0)$ and $f^* = f_i, i = 1, \ldots, m$.. Look for the best value of f_{best} according to (22). Set the particle corresponding to the best value of the objective function as the global best,$y_{Best}^{**}(0)$, with an objective function of f^{**}.

Step 2: *Time updating*: Update t = t + 1.
Step 3: *Velocity updating:* Update velocity by,

$$v_{i,k}(t) = w(t)v_{i,k}(t-1) + c_1 r_1 \left(y_{i,k}^*(t-1) - y_{i,k}(t-1) \right) + c_2 r_2 \left(y_{Best}^{**}(t-1) - y_{i,k}(t-1) \right). \quad (16)$$

Step 4: *Position updating:* Update the position of each particle by use of (30) and the value of updated velocity,

$$y_{i,k}(t) = y_{i,k}(t-1) + v_{i,k}(t). \quad (17)$$

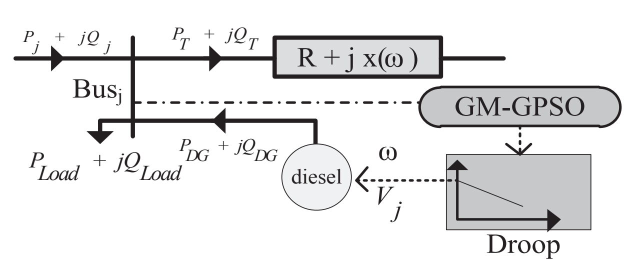

Fig. 3. Injected power of DGs to bus j based on droop.

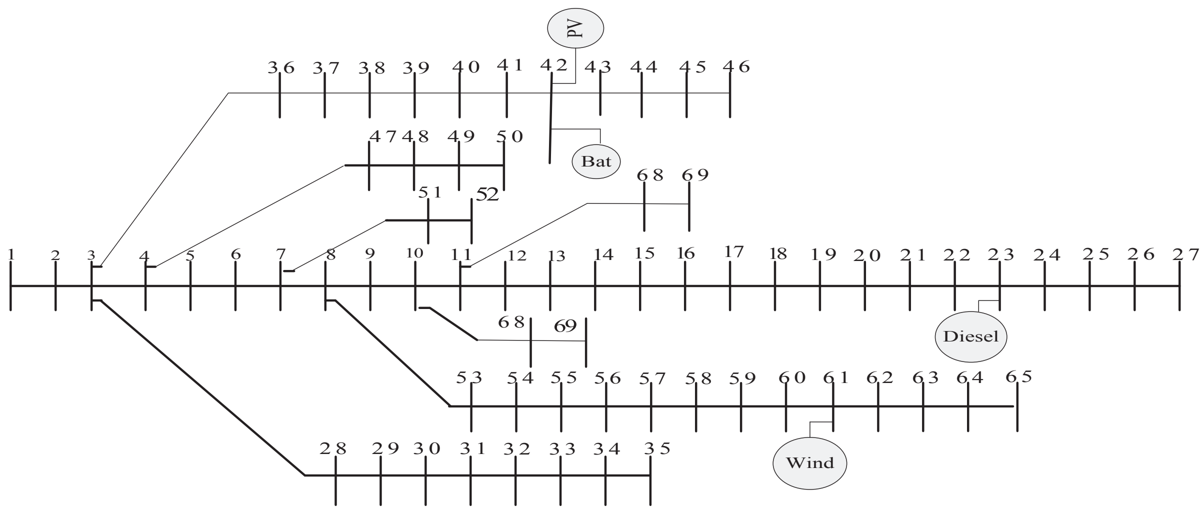

Fig. 4. 69-bus autonomous microgrid.

Step 5: *Gaussian mutation:* Mutate a new position at each swarm by use of mutation probability (P_n). Then, for each component of the particle position vector, $k = 1,\ldots, n$, if Rand (0,1) < P_n, then mutate component $y_{i,k\ (t)}$ by,

$$y_{i,k}(t) = y_{i,k}(t) + N(0,\sigma)y_{i,k}(t). \tag{18}$$

where standard deviation, σ, can be obtained by,

$$\sigma = 0.1(y_{max,k} - y_{min,k}). \tag{19}$$

Step 6: *Local updating*: If $f_{\min} < f^*$ then update individual best as, (noting that each particle is appraised based on the updated position),

$$y_i(t) = y_i^*(t), f_i = f_i^*. \tag{20}$$

Step 7: *Global improving:* Set ζ as the index of the global best particle, then update this particle by Refs. [27],

$$v_{\xi,k}(t) = -y_{\xi,k}(t-1) + y^{**}_{Best,k}(t-1) + wv_{\xi,k}(t-1) + \tau(t-1)(1-2r_2). \tag{21}$$

$$y_{\xi,k}(t) = y^{**}_{Best,k}(t-1) + wv_{\xi,k}(t) + \tau(t-1)(1-2r_2). \tag{22}$$

where $\tau(t)$ can be obtained by,

$$\tau(t) = \begin{cases} 2\tau(t-1) & \textit{if } \#\textit{successes}(t-1) > s_c \\ 0.5\tau(t-1) & \textit{if } \#\textit{failures}(t-1) > f_c \\ \tau(t-1) & \textit{otherwise} \end{cases}. \tag{23}$$

In (14), the notations “# successes” and “# failures” represent numbers of successes or failures, respectively. Here failure is meant$f(y^{**}_{Best}(t)) = f(y^{**}_{Best}(t-1))$.

Step 8: *Global updating:* If $f_{min} < f^{**}$ then update individual global best as $f^{**} = f_{min}$ and $y^{**}_{Best} = y_{\min}(t)$.

Step 9: *Stopping criterion:* If the considered stopping criterion is met, then end the calculation, otherwise go to Step 2.

To run the above proposed algorithm a new load flow algorithm is needed for droop based DGs as developed in the next section.

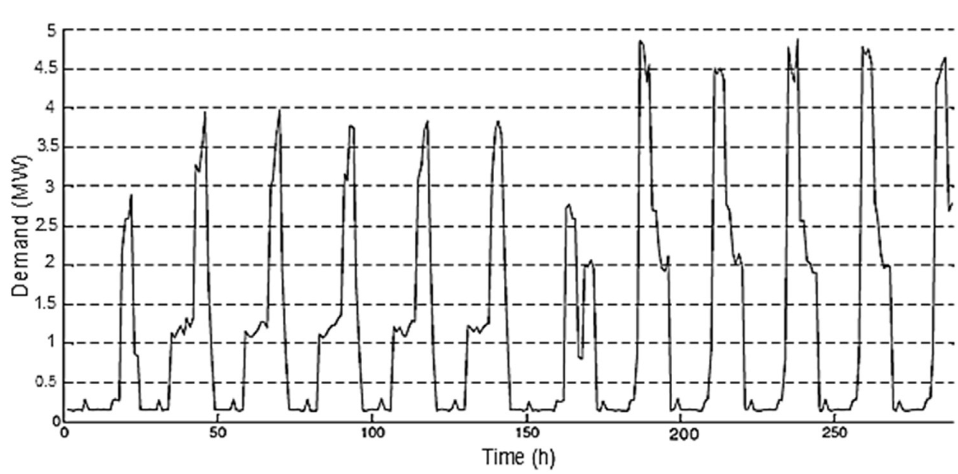

Fig. 5. Load pattern of 69-bus microgrid.

Table 1
GPSO-GM parameters.

Pop. size	$c_1 = c_2$	$r_1 = r_2$	w	$\rho(0)$	f_c	s_C	P_n
12	1	1	0.9	1.0	2	5	0.5

Table 2
Characteristics of different sources.

Characteristic	Type 1	2	3	4
a. Wind turbines				
V_{ci} (m/s)	3.5	3	2.5	3
V^{rated} (m/s)	13	12	10	7.4
V_{co} (m/s)	35	28	24	26
P_w^{rated}(kw)	2.4	5	10	25
Tower height (m)	10.6	14	18	27
Rotor diameter (m)	3.72	5.5	9.7	10.8
b. PV panels				
V^{max} (V)	17.6	17.8	18	18.3
P_w^{rated} (kw)	0.125	0.130	0.135	0.140
Efficiency (%)	16	16	16	16
Efficiency of inverter (%)	95	95	95	95
c. Battery banks				
V^{max} (V)	6	6	12	12
Capacity (Ah)	120	150	140	180
Efficiency (%)	85	85	85	85
Cost ($/$kw$)	348	415	521	567

4.2. Proposed load flow algorithm for autonomous microgrids

A load flow algorithm in the autonomous mode of the microgrid is developed here by considering that there is no slack bus in this mode therefore DGs, based on droop control, are required to participate in supplying loads to keep the microgrid frequency in its allowable range, while wind turbines, PV panels and battery banks are treated as constant power sources [17,29,30]. The algorithm steps are given as follows.

1) *Calculation for PQ buses:* The model of [31] is adopted and modified to calculate the magnitude and phase angle of bus voltage,

$$V_j^2 = \sqrt{\left(\left[rP_j + x(\omega)\cdot Q_j - \frac{V_i^2}{2}\right]^2 - \left[r^2 + x^2\right]\cdot\left[P_j^2 + Q_j^2\right]\right)} - \left[rP_j + x(\omega)\cdot Q_j - \frac{V_i^2}{2}\right] \quad (24)$$

$$\delta_j = \delta_i - \sin^{-1}\left(\frac{x(\omega)P_j - rQ_j}{V_i V_j}\right) \quad (25)$$

2) *Calculation for droop buses:* Unknown variables of a droop bus might be considered as active and reactive power as well as voltage magnitude and angle, as shown in Fig. 3. To calculate the phase angle of the receiving end bus, (20) is used where P_j and Q_j can be, respectively, obtained by,

$$P_j = -P_{diesel} + P_{load} + P_T \quad (26)$$

$$Q_j = -Q_{diesel} + Q_{load} + Q_T \quad (27)$$

It might be noticed that (21) and (22) are only applicable when P_j and Q_j are within their allowed ranges. In the case where the values of P_j and Q_j reach to their limits, they are considered as constant parameters with values equal to their limits. There follows the receiving end bus is converted from the droop control mode to the PQ mode. Therefore, the load flow problem needs to be resolved for the bus phase angle and voltage magnitude.

Two other equations used in droop bus calculation are (23) and (24) which are adopted for obtaining active and reactive power

Table 3
Best solution for 69-bus microgrid.

Source	Size (MW)	Inv. & Ins. Cost ($)	Gen. cost ($/year)	Maintenance cost ($/year)
PV	3.22	27351	0	127.34
Wind	4.83	682500	0	84286.15
Battery	12.8	160721.1454	0	0
Diesel	8.03	165735.7054	1638.7855	642.85

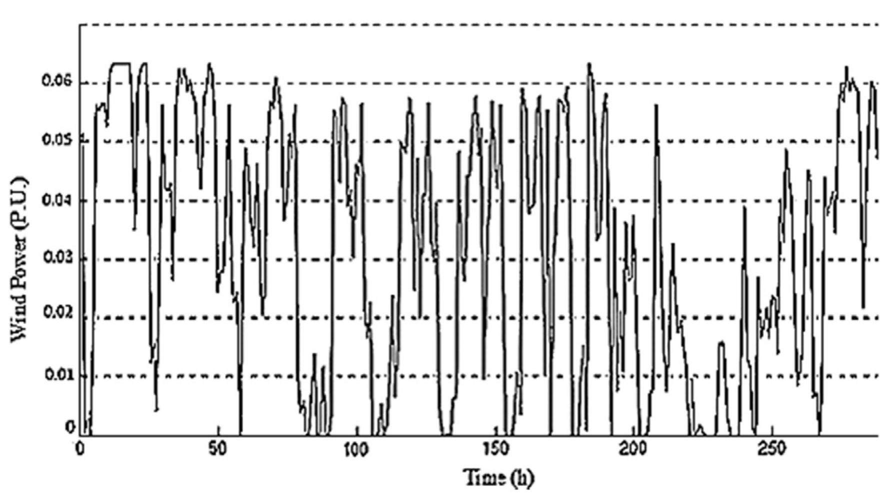

Fig. 6. Wind turbine power generation.

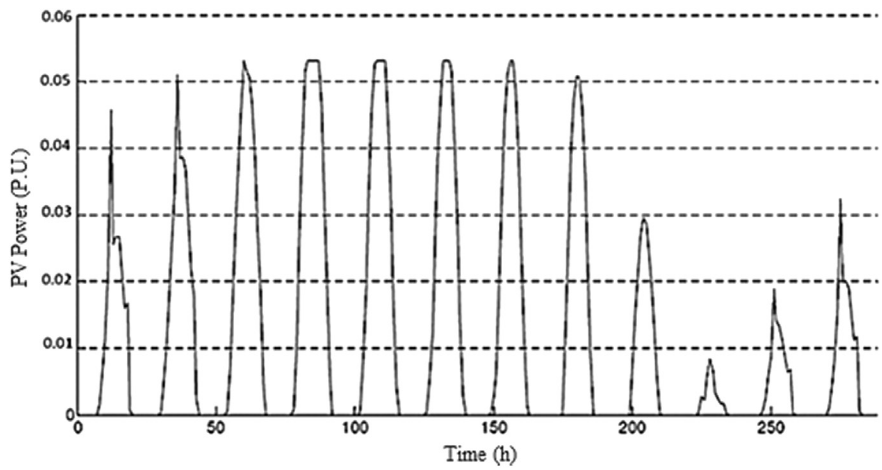

Fig. 7. Output power of PV panels.

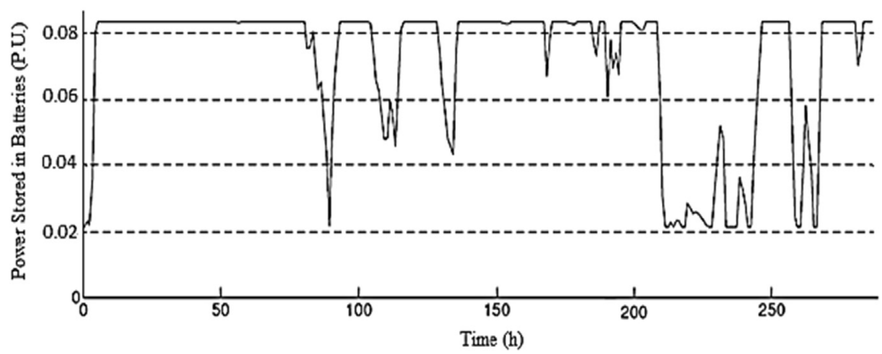

Fig. 8. Power stored in batteries.

sharing based on the frequency and local voltage of each DG, as given, respectively, by,

$$P_{dieseli} = \frac{1}{s_{pi}}(\omega_i^* - \omega) \quad (28)$$

$$Q_{dieseli} = \frac{1}{s_{qi}}\left(\left|V_i^*\right| - V_i\right) \quad (29)$$

5. Case studies

To assess the performance of the proposed method two case studies are considered.

5.1. A 69-bus microgrid

The first case study is a 69-bus autonomous microgrid, shown in Fig. 4, with data given in Ref. [28]. In this case, RESs are assumed to be located at buses 23, 42 and 61. The wind speed and solar irradiance data are obtained from Ref. [29]. A period of 20 years is considered for planning by considering the growth rate and then hourly load patterns are assigned to this period. For the illustration purpose, only one day of each month is considered in the simulation. The interest rate is assumed to be 20%. Fig. 5 gives the load pattern of this year and Table 1 shows the values of parameters used in GPSO-GM.

The capital investment, including installation costs, of the wind turbines, PV panels and the diesel generator are assumed to be of 1.96 $/MW, 5.1 $/MW and 0.87 $/MW their rated power, respectively [30] and their maintenance costs are of 3.05 $/MWh, 23 $/MWh and 1.02 $/MWh their output power, respectively. The operation cost of the diesel generator is assumed to be 0.5 $/MWh [30] and the PV area is considered to be restricted to 100 m^2. The lifetime of batteries is assumed to be 4 years [31]. The characteristics and costs of batteries are taken from Refs. [5], [31]. Table 2 summarizes characteristics of wind turbines, PV panels, and battery banks [5] and Table 3 summarizes the best solution obtained by the proposed method.

Table 4
A comparison between different methods for supplying load in 69-bus microgrid.

Scenarios	Source	Inv. & Ins. cost ($/year)	Gen. cost ($/year)	Maintenance cost ($/year)	Power cost ($/MWh)
1	Grid	1020109.897	29335.3537	4190.76	2.28
2	Diesel	35086.4212	20953.8241	8381.52	1.154
3	PV/Wind/Battery/Diesel	237629.7299	1638.7855	8266.18	0.63

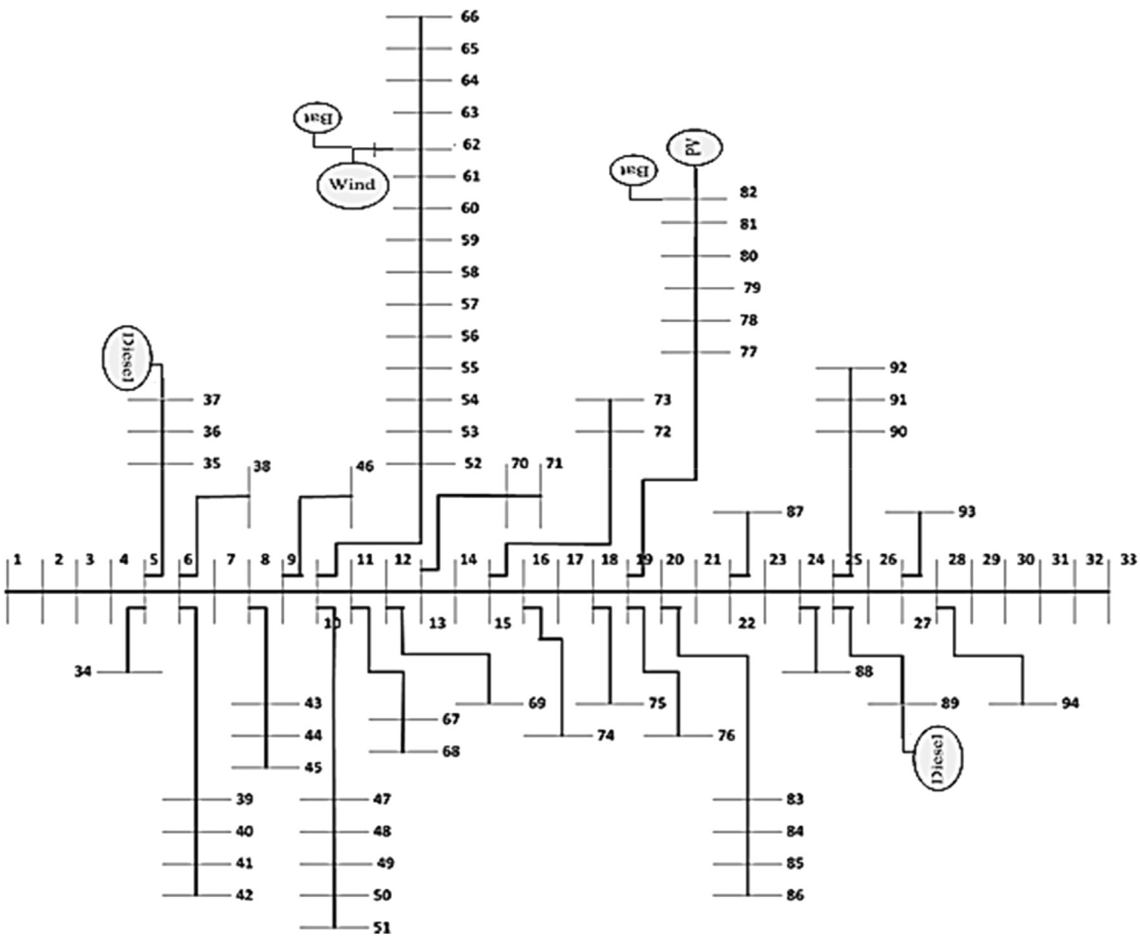

Fig. 9. 94-bus autonomous microgrid.

The values of power generation of the wind turbines, including 20 turbines (10 Type 3 and 10 Type 4), are shown in Fig. 6. As mentioned earlier the power generation of wind turbines depends on the wind speed at different hours of the planning horizon as well as their nominal power.

The values of power generation of the PV panels, including 43 panels (Type 2) are depicted in Fig. 7. The results in Figs. 6 and 7 show that there are periods in which the output power of the RESs is more than the load. The extra power in such periods, therefore, is stored in battery banks.

Fig. 8 illustrates the power stored in the battery banks. It should be noted that by considering $SOC_{Min} = 50\%$ as a constraint for the battery banks, only half of the power stored in them is available. In simulations, the initial value of SOC for the batteries is set at SOC_{Min}.

To examine the cost effective operation of the proposed method three scenarios are considered, as shown in Table 4. In the first scenario, it is assumed that the total microgrid's demand is provided by the main grid. In this scenario, the corresponding generation cost of power was obtained 29335.3537 $/year. In the second scenario, it is considered that the total demand is supplied by the diesel. The generation cost was obtained 20953.8241 $/year in this scenario. Finally, in the third scenario, a hybrid of RESs and diesel

Table 5
Best solution of optimization problem for 94-bus microgrid.

Source	Size (MW)	Inv. & Ins. cost($)	Gen. cost ($/year)	Maintenance cost ($/year)
PV	4.51	35282	0	133.65
Wind	5.06	726053	0	91148.08
Battery	15.84	205307.62	0	0
Diesel	9.54	186348.55	1736.57	703.62

Table 6
A comparison between different methods for supplying MG's load in 94-bus microgrid.

Source	Power cost ($/MWh)	Gen. cost ($/year)	Maintenance cost ($/year)
Grid	3.86	35174.52	4387.35
Diesel	1.64	23715.75	9527.52
PV/wind/battery/diesel	0.85	1894.04	8429.04

Table 7
Total cost ($/year) of 69-bus microgrid calculated by different algorithms.

Algorithms	SD (%)	BM	WV	Ave Time (min)
GA	2.06	250571.45	265481.42	20.58
PSO	1.83	253862.63	267041.53	16.03
GPSO-GM	1.04	247533.32	250612.74	15.47

along with battery banks are considered for supplying the total demand of microgrid. In this scenario, the generation cost was obtained 1638.7855 $/year. A comparison between these three scenarios shows that the operation in the proposed method is more cost effective than the other methods. The results, in Table 4, also illustrate that the first and third scenarios have, respectively, largest and lowest maintenance costs. In addition, the results demonstrate that using both battery banks and diesel generators simultaneously is effective in supporting renewable resources.

5.2. A 94-bus microgrid

The second case study is an actual Portuguese network with 94 buses, as shown in Fig. 9 [33]. In this case, the RESs are assumed to be located at buses 62 and 82, and two diesels are considered at buses 37 and 89. The wind turbines are assumed to have 20 turbines of Types 3 and 4. Also, the PV panels are considered to have 52 panels of Type 2.

The best solution obtained by the proposed method is provided in Table 5 and Table 6, comparing different methods for supplying microgrid's power, provides support for the cost effectiveness of the proposed hybrid system. Although the maintenance cost of the proposed hybrid system is higher than the grid, this might be disregarded in comparison with the generation cost. The results also support use of battery banks and diesel generators simultaneously as an optimum design for supporting renewable resources.

6. Discussion

6.1. Optimal capacity of subsystems

Care needs to be exercised in selecting the optimal capacity of subsystems for supplying the microgrid's demand. For example, Table 3 shows that the investment cost of PV panels is low. So one may consider a higher capacity for such panels; however, a reliability problem arises as PV works based on solar radiation which generally varies in different seasons (see Fig. 7). Similar happens to wind turbines. Diesel generators may therefore contribute mostly in power generation for example, in fall and winter seasons due to low solar irradiance and wind speed.

6.2. Optimization method

Two operators, Gaussian mutation and guaranteed convergence, used in the proposed optimization algorithm, GPSO-GM, helps in providing accurate results compared with other conventional methods (PSO and GA). To assess the performance of GPSO-GM a numerical analyze for a 69-bus microgrid was carried out for comparing the performance of GOSO-GM with that of GA and PSO. After 40 runs of each algorithm, the standard deviation (SD), worst value (WV), best mean (BM) of the objective function, (15), and the average calculation time (Ave Time) were obtained with the parameters of GA and PSO determined from Ref. [32]. The corresponding results are summarized in Table 7. The population size for all algorithms was assumed to be 12. The BM values show the convergence ability of the algorithms and a small standard deviation demonstrates the stability and better convergence of them. The results show that GPSO-GM provides the lowest SD, BM, WV and Ave Time compared with other algorithms. This proves the robustness and accuracy of GPSO-GM in obtaining the solution.

7. Conclusion

This paper developed an optimal strategy for supplying required energy in an autonomous microgrid by the means of a hybrid energy system, including PV, wind, battery banks and diesel generators based on operational and financial perspectives. The development focused on maximizing the contribution of renewable sources in energy supply. An optimization problem was formulated and a new algorithm, GPSO-GM, was presented to solve the optimization problem. The simulation results showed the effectiveness of the proposed strategy in finding the optimum design. The results also showed the proposed hybrid system is capable to meet the electricity demand of the microgrid. Moreover, the economic evaluation suggested the proposed system as a preferable investment compared with other alternatives. In addition, the results illustrated that the design of hybrid energy systems based on using both battery banks and diesel generators to support renewable resources is more effective than the design which only uses solely diesel generators or battery banks. Finally, the accuracy and robustness of GPSO-GM compared with other conventional algorithms were shown. Although this paper mainly concentrated on economic evaluation of hybrid energy systems examining other aspects of the sustainability of these systems, such as social, can be subject of the future research.

References

[1] B.K. Bala, S.A. Siddique, Optimal design of a PV/Diesel hybrid system for electrification of an isolated island Sandwip in Bangladesh using genetic algorithm, Energy Sustain. Dev. 13 (2009) 137–142.

[2] M. Muselli, G. Notton, A. Louche, Design of hybrid-photovoltaic power generator, with optimization of energy management, Sol. Energy 65 (1999) 143–157.

[3] B.R. Bagen, Evaluation of different operating strategies in small stand-alone power systems, IEEE Trans. Energy Convers. 20 (2005) 654–660.

[4] M.K. Deshmukh, S.S. Deshmukh, Modeling of hybrid renewable energy systems, Renew. Sustain. Energy Rev. 12 (2008) 235–249.

[5] M. Eroglu, E. Dursun, S. Sevencan, J. Song, S. Yazici, O. Kilic, A mobile renewable house using PV/wind/fuel cell hybrid power system, Int. J. Hydrogen Energy 36 (2011) 7985–7992.

[6] S. Colle, S.L. Abreu, R. Ruther, Economic evaluation and optimization of hybrid diesel/photovoltaic systems integrated to electricity grid, Sol. Energy 76 (2004) 295–299.

[7] W. Zhou, C. Lou, Z. Li, L. Lu, H. Yang, Current status of research on optimum sizing of stand-alone hybrid solar–wind power generation systems, Appl. Energy 87 (2010) 380–389.

[8] D. Saheb-Koussa, M. Haddadi, M. Belhamel, Economic and technical study of a hybrid system (wind–photovoltaic–diesel) for rural electrification in Algeria, Appl. Energy 86 (2009) 1024–1030.

[9] D. Weisser, A guide to life-cycle greenhouse gas (GHG) emissions from electric supply technologies, Energy 32 (2007) 1543–1559.

[10] G. Bekele, G. Tadesse, Feasibility study for a standalone solar–wind-based hybrid energy system for application in Ethiopia, Appl. Energy 87 (2010) 487–495.

[11] S. Diaf, G. Notton, M. Belhamel, M. Haddadi, A. Louche, Design and techno-economical optimization for hybrid PV/wind system under various meteorological conditions, Energy 85 (2008) 968–987.

[12] M. Kalantar, G.S.M. Mousavi, Dynamic behavior of a stand-alone hybrid power generation system of wind turbine, microturbine, solar array and battery storage, Appl. Energy 87 (2010) 3051–3064.

[13] H.X. Yang, L. Lu, W. Zhou, A novel optimization sizing model for hybrid solar-wind power generation system, Sol. Energy 81 (2007) 76–84.

[14] S. Rehman, M. Alam, J.P. Meyer, L.M. Al-Hadhrami, Feasibility study of a wind-pv-diesel hybrid power system for a village, Renew. Energy 38 (2012) 258–268.

[15] E.M. Nfah, J.M. Ngundam, M. Vandenbergh, J. Schmid, Simulation of off-grid generation options for remote villages in Cameroon, Renew. Energy 33

(2008) 1064–1072.
[16] S. Gomaa, A.K.A. Seoud, H.N. Kheiralla, Design and analysis of photovoltaic and wind energy hybrid systems in Alexandria, Egypt Renew. Energy 6 (1995) 643–647.
[17] G. Carpinelli, P. Caramia, P. Varilone, Multi-linear Monte Carlo simulation method for probabilistic load flow of distribution systems with wind and photovoltaic generation systems, Renew. Energy 64 (2015) 1221–1228.
[18] M. Mikati, M. Santos, C. Armenta, Electric grid dependence on the configuration of a small-scale wind and solar power hybrid system, Renew. Energy 57 (2013) 587–593.
[19] T. Ma, H.X. Yang, L. Lu, J.Q. Peng, Pumped storage-based standalone photovoltaic power generation system: modeling and techno-economic optimization, Appl. Energy 137 (2015) 649–659.
[20] O. Ekren, B.Y. Ekren, Size optimization of a PV/wind hybrid energy conversion system with battery storage using simulated annealing, Appl. Energy 87 (2010) 592–598.
[21] A. Evans, V. Strezov, T.J. Evans, Assessment of sustainability indicators for renewable energy technologies, Renew. Sustain Energy Rev. 13 (2009) 1082–1088.
[22] A. Stoppato, Life cycle assessment of photovoltaic electricity generation, Energy 33 (2008) 224–232.
[23] M.H. Moradi, M. Abedini, S.M. Hosseinian, Improving operation constraints of microgrid using PHEVs and renewable energy sources, Renew. Energy 83 (April) (2015) 543–552.
[24] E. Koutroulis, D. Kolokotsa, A. Potirakis, K. Kalaitzakis, Methodology for optimal sizing of stand-alone photovoltaic/wind-generator systems using genetic algorithms, Sol. Energy 80 (2006) 1072–1088.
[25] E. Alsema, M De Wild-Scholten, Environmental impact of crystalline silicon photovoltaic module production, in: Material Research Society Fall Meeting, Symposium G: Life Cycle Analysis Tools for "green" Materials and Process Selection, Boston, MA, 2005.
[26] G. Notton, M. Muselli, A. Louche, Autonomous hybrid photovoltaic power plant using a back-up generator: a case study in a Mediterranean Island, Renew. Energy 7 (1996) 371–391.
[27] M. Sharafi, Tarek Y. ELMekkawy, multi-objective optimal design of hybrid renewable energy systems using PSO-simulation based approach, Renew. Energy 68 (2014) 67–79.
[28] B. Venkatesh, R. Ranjan, Data structure for radial distribution power flow analysis, IEE 150 (2003) 101–106.
[29] E. Skoplaki, J.A. Palyvos, Operating temperature of photovoltaic modules: a survey of pertinent correlations, Renew. Energy 34 (2009) 23–29.
[30] P.A. Daly, J. Morrison, Understanding the potential benefits of distributed generation on power delivery systems, in: Rural Electric Power Conference, 2001, pp. 201–213.
[31] Phaesun stand-alone solar solution, Product Catalogue: Photovoltaic and Wind Generators, 2009.
[32] M.H. Moradi, M. Abedini, A combination of genetic algorithm and particle swarm optimization for optimal DG location and sizing in distribution systems, Int. J. Elect. Power Energy Syst. 34 (1) (Jan.2012) 66–74.
[33] Zeinalzadeh Arash, Mohammadi Younes, M.H. Moradi, Optimal multi objective placement and sizing of multiple DGs and shunt capacitor banks simultaneously considering load uncertainty via MOPSO approach, Int. J. Elect. Power Energy Syst. (67) (2015) 336–349.

Nomenclature

C_{wind}: sum of operational and maintenance costs of wind turbines
C_{PV}: sum of operational and maintenance costs of PV panels
C_{diesel}: sum of operational and maintenance costs of diesels
$C_{battery}$: sum of operational and maintenance costs of batteries
S_i: surface of one PV (m^2)
$I_r(t)$: solar irradiance in W/m^2 in hour t
InfR, IntR: inflation rate (9%) and interest rate (12.5%),respectively.
ins: index of installation cost
inv: index of investment
st: standard test conditions
f^{PV}: derating factor for PV panels
α^{PV}: temperature coefficient of PV panels
m: index of maintenance costs
v^{rated}: wind speed
v_r: wind speed in the reference height
v_{co}: cut-out speed
SOC_{min}: minimum state of charge (50%)
V_{DC}: DC bus voltage
$V_{battery}^{rated}$: nominal voltage of each battery
c_1, c_2: weighting factors
$w(t)$: inertia weighting coefficient
y: year index
T_C: temperature of PV panels
T: time in the planning horizon
ζ: index of global best particle
r_1, r_2: weighting factors
S_C, f_C: number of successes or failures, respectively
σ: standard deviation
V^*: nominal value of voltage magnitude
r_i, x_i: resistance and reactance of branch *I*, respectively
S_p, S_q: active and reactive power static droop gains, respectively
δ: phase angle
ω^*,ω: nominal and operational values of frequency, respectively
P_{load}, Q_{load}: active and reactive power demand at the receiving end bus, respectively
P_T, Q_T: total active and reactive power of bus *j*, respectively
P_{Bat}: achievable power of battery banks
P_{wind}: output of wind turbines
P_{PV}: output of PV panels
p_w^{rated}: power output of the wind turbine
Δ_t: length of time interval *t* (hours)
T: set of time intervals
η^{PV}: PV panels efficiency
γ: power law exponent (1/5)
η_{inv}: inverter efficiency